Adsorption in a spherical cavity

Douglas Henderson and Stefan Sokołowski*
Departamento de Física, Universidad Autónoma Metropolitana, Apartado Postal 55-534, 09340 Distrito Federal, México
(Received 12 October 1994)

This paper reports on studies of adsorption in spherical cavities of different sizes. The calculations have been carried out by the density functional approach. We have studied the influence of the cavity size and attractive particle-cavity forces on the phase behavior of confined fluids. We find that capillary condensation occurs. As the radius of the cavity is decreased, the transition is shifted toward lower densities of the bulk fluid, which is in equilibrium with the fluid in the cavity.

PACS number(s): 68.45.−v, 68.10.−m

I. INTRODUCTION

In recent years significant progress has been made in understanding fluid behavior in contact with planar walls and in pores of planar or cylindrical geometry [1–10]. Recently, there has also been growing interest in other geometries involving cases of geometrically nonuniform walls and pores [7,11–18]. This is because such systems are not only related to various important practical processes, but they also exhibit a rich variety of phase behavior. However, the problem of nonplanar interphases is still far from being complete. By this, we mean problems involving not only spherical cavities, but also adsorption on colloidal particles. Note that the adsorption in spherical cavities has been studied previously in Refs. [7,13–15] by using both theoretical approaches and computer simulations. There are also theoretical works devoted to the problem of a description of fluids inside of spherical vesicles [19].

The usual approaches to the study of porous systems have been based on either computer simulations or integral equations or density functional theories [1,2,7,14]. Among the usual techniques in liquid theory, density functional theories [2,7(b),20] have been shown to be both computationally simple and reliable for the description of simple liquids in the inhomogeneous phase. For this case, the most successful density functional theories are those which involve a coarse-grained average density. One should perhaps mention here that, to our knowledge, one of the first nonlocal density functional expansions for the direct correlation function was proposed in Ref. [21].

In this work we study adsorption in spherical cavities. One of the important questions we consider is how the size of cavities affects adsorption and the transitions in adsorbed layers, e.g., capillary condensation and surface wettability. The theoretical description is based on the equation for the density profile developed from the Evans and Tarazona [2,20] version of the density functional approach, which has been proved to be successful for treating adsorption at planar interphases and in slitlike and cylindrical pores, at least when simple fluids are considered. The main goal of the calculations performed here is to apply this theory to the case of adsorption of a Lennard-Jones fluid inside of a cavity with repulsive-attractive walls. The fluid inside the cavity is assumed to be in equilibrium (i.e., at the same chemical potential) with a bulk fluid. In practice, this could be achieved by means of a hole in the cavity wall. The mechanism for achieving this equilibrium is not specified in our formalism. We assume only that the spherical symmetry is not affected.

II. THEORY

Let us consider [2] the definition of the grand potential Ω:

$$\Omega = F + \int d\mathbf{r}\, n(\mathbf{r})[v(\mathbf{r}) - \mu] , \tag{1}$$

where μ is the chemical potential, $n(\mathbf{r})$ is the inhomogeneous density, and $v(\mathbf{r})$ is the fluid-solid interaction potential. We divide the functional F into two parts: the contributions due to the repulsive forces and the attractive forces between the molecules, F_R and F_A, respectively. The former contribution is modeled by hard spheres with a suitable diameter d and the latter contribution is treated in a mean-field approximation. To calculate F_R, a smoothed nonlocal density function $\bar{n}(\mathbf{r})$ is introduced,

$$\bar{n}(\mathbf{r}) = \int d\mathbf{r}' n(\mathbf{r}') w(|\mathbf{r} - \mathbf{r}'|, n(\mathbf{r})) , \tag{2}$$

where w is a weight function. This function is assumed to be described by a power series expansion

$$w(r,n) = w_0(r) + w_1(r)n + w_2(r)n^2 , \tag{3}$$

and the coefficients w_0, w_1, and w_2 are given by Tarazona [19]. The free energy then takes the form

$$F = \int d\mathbf{r}\, n(\mathbf{r})\{kT[\ln n(\mathbf{r})\lambda^3 - 1] + f(\bar{n}(\mathbf{r}))\} + \tfrac{1}{2}\int d\mathbf{r}\, d\mathbf{r}' n(\mathbf{r}) n(\mathbf{r}') u_A(|\mathbf{r} - \mathbf{r}'|) , \tag{4}$$

where λ is the thermal wavelength, u_A is the attractive part of the interparticle potential, and f is the free-energy

*Permanent address: Computer Laboratory, Department of Chemistry, MCS University, 20031 Lublin, Poland.

density of a hard-sphere fluid. To calculate f the Carnahan-Starling equation [22] is used:

$$f(n)/kT=\eta(4-3\eta)/(1-\eta)^2 , \quad (5)$$

where $\eta=\pi d^3 n_0/6$ is the packing fraction and n_0 is the bulk fluid density.

The equilibrium density profile minimizes the grand potential Ω; thus the local density is evaluated from the condition [2,20]

$$\delta\Omega[n(\mathbf{r})]/\delta n(\mathbf{r})=0 . \quad (6)$$

This gives the integral equation for the density profile. As usual, the excess adsorption isotherm Γ is defined by the equation

$$A\Gamma=\int d\mathbf{r}[n(\mathbf{r})-n_0] , \quad (7)$$

where A is the area; the integration is performed over the entire volume available to particles of the fluid and n_0 is the density of a uniform system having the same chemical potential as the fluid in the cavity. For example, as already mentioned, this uniform fluid might be a fluid outside the cavity and "connected" to the fluid in the cavity by a small hole.

III. RESULTS AND DISCUSSION

In this work we consider a Lennard-Jones fluid with a cutoff:

$$u(r)=\begin{cases}4\varepsilon[(\sigma_s/r)^{12}-(\sigma_s/r)^6] & \text{for } r\le r_c \\ 0 & \text{for } r>r_c ,\end{cases} \quad (8)$$

where the cutoff distance r_c has been assumed to be $r_c=2.5\sigma_s$. The division of the potential $u(r)$ we employ here,

$$u_A(r)=\begin{cases}-\varepsilon & \text{for } r\le 2^{1/6}\sigma_s \\ u(r) & \text{for } r>2^{1/6}\sigma_s ,\end{cases} \quad (9)$$

has been used in some density functional calculations [2,11,12]. The reference hard-sphere diameter is σ_s. We have assumed that ε/k and σ are those characteristic for argon, i.e., $\varepsilon/k=120$ K and $\sigma=3.4$ Å. Without loss of generality, we can also use σ as a unit of length.

To calculate the attractive interaction between the cavity and a fluid particle, we assume that the surface of the cavity is "divided" into attractive elements smeared on the surface. Therefore we perform an integral over the whole set of attractive elements given by

$$v(R)=\int_S (4\varepsilon_{ls}[\{\sigma_{ls}/\Sigma(\mathbf{r})\}^{12}-\{\sigma_{ls}/\Sigma(\mathbf{r})\}^6])d\mathbf{r} , \quad (10)$$

where ε_{ls} and σ_{ls} are the potential parameters, R is the distance from the center of the cavity, and $\Sigma(\mathbf{r})$ is the distance from the point $(0,0,R)$ to a point on the surface of the cavity of diameter σ_l. In the case of a planar surfaces (i.e., when $\sigma_l\to\infty$) the last equation leads [23] to the well-known Lennard-Jones (10,4) function. In all our calculations we have assumed that $\sigma_{ls}=0.9$.

The method of solution of the density profile equation was based upon a standard iterational procedure. Note that at some values of the chemical potential, corresponding to the bulk or uniform fluid which is in equilibrium with the confined fluid, multiple solutions are possible. Obviously, the thermodynamically stable solution should correspond [2] to the minimum of Ω. In the cases which we have investigated, at some thermodynamic conditions of bulk density and the temperature, two solutions of Eq. (6) have been found. At a constant temperature we plot the grand potential Ω versus the bulk density (cf. Ref. [24]). Obviously in the transition region this plot consists of two intersecting curves; the intercept of these two branches determines the equilibrium transition point. The above procedure is equivalent to the classical Maxwell construction for a given step in the adsorption isotherm [23].

It is well known that the fluid confinement of the fluid leads to a shift of the fluid-gas coexistence curves towards lower values of the chemical potential. This phenomenon is known as a capillary condensation [3–12]. In addition to including capillary condensation, confinement affects other possible transitions in the structure of surface film, such as layering and wetting transitions.

Before discussing the results, we should note that the mean-field approach for attractive interparticle forces enforces the possible transitions. For example, it is well known that for one-dimensional systems the theory which is the counterpart of that used here leads to unphysical results, i.e., to the prediction of a first-order liquid-gas transition. In the case of a real fluid confined in a spherical cavity, the system always has a finite size and, consequently, discontinuous jumps in the adsorption isotherms should become smooth with inflexion points. By comparing the predictions of the present approach for a such case one defines eventually the location of the inflexion point as the characteristic point.

In Figs. 1, 2, and 3 we show examples of the density profiles obtained for the cavity of diameter 20. The curves given in Fig. 1 were evaluated for $\varepsilon_{ls}/k=300$ K. In the case of the curves given in Fig. 2 the adsorbing potential was lower and $\varepsilon_{gs}/k=200$ K. The lowest adsorbing potential $\varepsilon_{gs}/k=100$ K is for the case of the curves presented in Fig. 3. Figure 4 shows examples of the adsorption isotherms evaluated from the density profiles.

Depending on the strength of the cavity-particle energy, and on the temperature, different scenarios occur for the pore filling. When the temperature is low enough and the adsorbing potential high, the "condensation" occurs in the inner part of the pore. The number of layers completed before condensation is 5–6 [see Fig. 1(a)]. In this case the filling of the subsequent layers is manifested as a series of "continuous steps" leading to a final discontinuity in the adsorption isotherm (see Fig. 4). We know [2] that at a still lower temperature, a higher adsorbing potential, and when $\sigma_l\to\infty$, i.e., for a planar wall, the theory would lead to a discontinuous filling of the sequence of layers in $n(\mathbf{r})$. This phenomenon is known as the "layering transition" [2]. Finite curvature of the surface rounds these transitions [25,26].

When the temperature increases, the stepwise character of the adsorption isotherm becomes less visible (see Fig. 4) and there are only three first layers adjacent to the

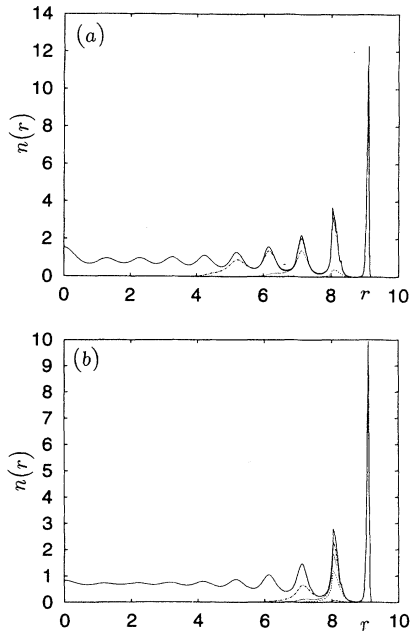

FIG. 1. The density profiles in the spherical cavity of diameter $\sigma_l=20$. The energy parameter $\varepsilon_{ls}/k=300$ K and the temperature to (a) 84 K and (b) 100 K. The curves (in order from the bottom) in (a) were calculated for $n_0=0.0005$, 0.000 12, 0.000 14, and 0.0020. The curves (in order from the bottom) in (b) are for $n_0=0.001$, 0.002, 0.003, and 0.004, and 0.007.

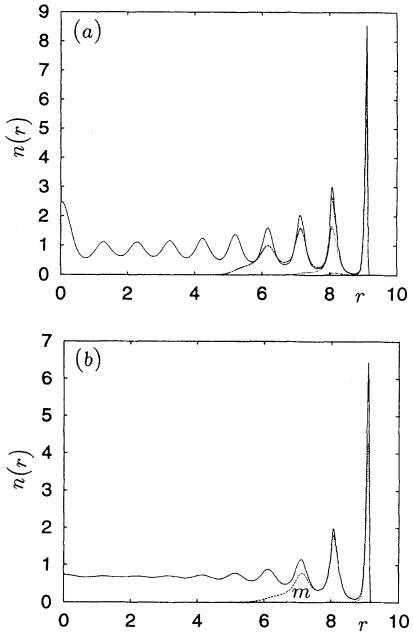

FIG. 2. The density profiles in the spherical cavity of diameter $\sigma_l=20$. The energy parameter ε_{ls}/k was equal to 200 K and the temperature to (a) 84 K and (b) 100 K. The curves (in order from the bottom) in (a) were calculated for $n_0=0.0002$, 0.000 12, 0.000 15, and 0.0022. The curves (in order from the bottom) in (b) are for $n_0=0.002$, 0.006, and 0.0075. The curve marked by m corresponds to a metastable state.

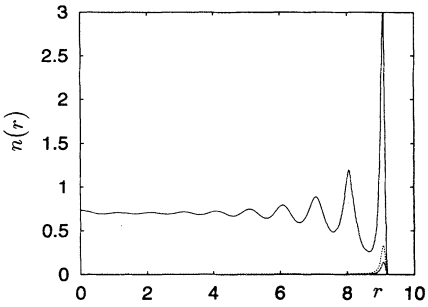

FIG. 3. The density profiles in the spherical cavity of diameter $\sigma_l=20$. The energy parameter ε_{ls}/k was equal to 100 K and the temperature to 100 K. The curves (in order from the bottom) were calculated for $n_0=0.002$, 0.004, and 0.008.

cavity wall before the "condensation" is completed [see Fig. 1(b)].

In the case of a "weaker" surface at low temperatures, the number of "completed" layers before the "condensation point" decreases [see Fig. 2(b)]. When the temperature also increases, only the first layer adjacent to the cavity wall is filled before "condensation" [Fig. 2(b)]. The density profile marked by the label "m" in Fig. 2(b) corresponds to the metastable situation.

With a subsequent decrease of the adsorbing potential, further characteristic changes occur (see Fig. 3). Before rapid condensation inside of the whole pore, only a thin film at the surface of the cavity is developed. In the case of adsorption on a planar wall, the adsorbed film may undergo the so-called thin-thick film transition, or prewet-

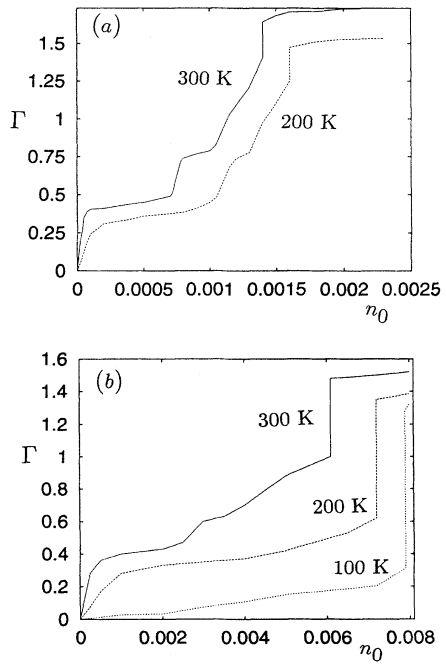

FIG. 4. Adsorption isotherms in a spherical cavity of diameter $\sigma_l=20$ at (a) $T=84$ K and (b) $T=100$ K. The numbers 100, 200, and 300 denote the values of the energy parameter ε_{ls}/k.

ting transition [2,27]. For adsorption in slitlike pores a competition between prewetting and capillary condensation can be also observed [24]. In the case of any finite curvature, the prewetting transitions are smeared out; the nonzero curvature of the wall acts as "an external field" shifting the observer away from the transition at zero curvature [25,26]. Nevertheless, when the cavity is large, we can expect from the theory the presence of a continuous jump, corresponding to the prewetting transition in the limit $\sigma_l \to \infty$. In the case of the curves given in Fig. 3 it is very difficult to check whether the film fills the whole cavity or only a part of it and if there is another step in the adsorption isotherm, connected with the filling of the remaining part of the pore. Our calculations suggest rather the existence of a single step on the adsorption isotherm, connected with "condensation."

Note that for a low temperature and a high chemical potential (or density) of bulk gas, which is in equilibrium with the fluid inside the cavity, the density profile exhibits a series of well-developed peaks, indicating the formation of an "ordered" structure inside the cavity [see Fig. 2(b), for example]. In such a case the peak at the pore center can grow and become higher than the outermost peaks. Obviously, this is connected with the existence of a rather high potential field at the pore center, which is created by the "ordered" confined phase.

When the size of the cavity decreases, the adsorbing potential becomes stronger. Obviously, this effect is significant for small cavities. In such a case, all the above described phenomena are shifted towards lower bulk gas densities. When the cavity is still "large" in comparison with the molecules of the fluid, the height of the first peak adjacent to its wall is almost unchanged. The most visible changes occur at the cavity center. Because the whole system becomes more "ordered," the central peak increases significantly.

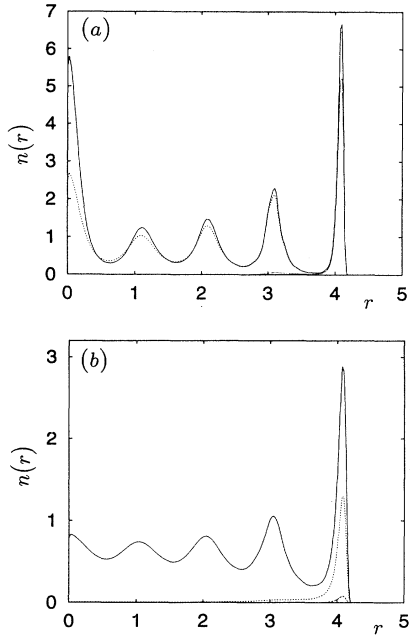

FIG. 5. The density profiles in the spherical cavity of diameter $\sigma_l = 10$. The energy parameter ε_{ls}/k was equal to (a) 200 K and (b) 100 K. The temperature is 100 K. The curves (in order from the bottom) in (a) were calculated for $n_0 = 0.002$, 0.007, and 0.008, whereas in (b) they were calculated for $n_0 = 0.001$, 0.004, and 0.008.

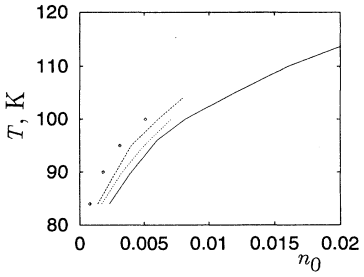

FIG. 6. Examples of the evaluated phase diagrams. The solid line is the bulk dew line and the dotted lines (from the bottom) are the parts of the capillary condensation line calculated for $\sigma_l = 10$ and for $\varepsilon_{ls}/k = 200$ and 300 K, respectively. The points were evaluated for $\varepsilon_{ls}/k = 300$ K, but pore $\sigma_l = 10$.

Figures 5(a) and 5(b) show examples of the density profiles evaluated for the cavity having the diameter 10. The potential parameter ε/k was equal to 200 and 100 K, respectively. Figure 5(a) should be compared with Fig. 2(b) and Fig. 5(b) should be compared with Fig. 3. Whereas before "condensation" the heights of the first peaks in Figs. 2(b) and 5 are similar, the heights of the same peaks in Figs. 3 and 5(b) are different. This illustrates that even small changes in the adsorbing potential can influence the structure of the adsorbed film.

Finally in Fig. 6 we present examples of a part of the phase diagram evaluated for the investigated systems. The solid line is the dew line of the bulk system. All remaining lines and points corresponding to the jumps in the adsorption isotherm, which we treat as a "capillary condensation." Recall that the method of their evaluation has been briefly described above; it was identical with that presented in Ref. [24]. The confinement leads to the shift of the line towards lower bulk gas densities. This shift is bigger when the size of the pore decreases and when the adsorbing potential increases. Note that only parts of the diagrams for confined systems are presented here.

IV. CONCLUSIONS

Before concluding it is necessary to make some comments concerning the theoretical model. To perform our calculations we have used an approach involving a mean-field treatment of the attractive interparticle forces. One well-known consequence for the bulk fluid, which is in equilibrium with the investigated system, is a shift of the critical point to higher temperatures. In addition, the location of the transition point and the shape of the coexistence line of the bulk fluid are different from those obtained from more refined theoretical models which take molecular correlations into account. Of course, the results presented here also suffer from these limitations. As we have stressed above, because of the finite size of the

systems under study, we expect that the "condensation" in an experimental system should occur continuously.

In this paper the usual density functional approach for an inhomogeneous fluid has been extended to study the adsorption of a fluid in a spherical cavity. We find that many of the effects observed for the adsorption of a fluid at a flat surface and slitlike pores are also present in the spherical cavity. In particular, as the density increases, layering in the density profile occurs with an abrupt "condensation" of the fluid. Decreasing the radius of the cavity shifts the transition towards lower densities of the bulk fluid in equilibrium with the fluid in the cavity. Further studies are possible. However, the main features of adsorption in a spherical cavity have been pointed out.

ACKNOWLEDGMENTS

The authors wish to express gratitude to the CONACYT of Mexico (Grant No. 4186-E9405 and el Fondo para Cátedras Patrimoniales de Excelencia) for financial support of the project. They also thank Dr. Orest Pizio, Instituto de Química, UNAM and Dr. M. Wortis, Department of Physics, SFU for valuable discussions.

[1] D. Henderson, in *Fundamentals of Inhomogeneous Fluids,* edited by D. H. Henderson (Marcel Dekker, New York, 1992).
[2] R. Evans, in *Fundamentals of Inhomogeneous Fluids* (Ref. [1]).
[3] S. Sokolowski and J. Fischer, J. Chem. Phys. **93**, 6787 (1991).
[4] P. C. Ball and R. Evans, Mol. Phys. **63**, 159 (1988).
[5] A. Papadopoulou, F. van Swol, and U. M. B. Marconi, J. Chem. Phys. **92**, 6942 (1992).
[6] E. Kozak and S. Sokolowski, J. Chem. Soc. Faraday Trans. I **87**, 3415 (1991).
[7] (a) Y. Zhou and G. Stell, Mol. Phys. **66**, 767 (1989); (b) J. Chem. Phys. **92**, 5533; **92**, 5544 (1990).
[8] M. Schoen, D. J. Diestler, and J. H. Cushman, J. Chem. Phys. **87**, 5464 (1987).
[9] W.-J. Ma, J. R. Banavar, and J. Koplik, J. Chem. Phys. **97**, 485 (1992).
[10] R. D. Kaminski and P. A. Monson, J. Chem. Phys. **95**, 2936 (1991).
[11] G. Chmiel, K. Karykowski, W. Rżysko, A. Patrykiejew, and S. Sokolowski, Mol. Phys. **81**, 691 (1994).
[12] G. Chmiel, L. Łajtar, S. Sokołowski, and A. Patrykiejew, J. Chem. Soc. Faraday Trans. II **90**, 1153 (1994).
[13] J. Stecki and S. Toxvaerd, J. Chem. Phys. **93**, 7342 (1990).
[14] A. Samborski, J. Stecki, and A. Poniewierski, J. Chem. Phys. **98**, 5442 (1993).
[15] Soon-Chul Kim, Je-Kwan Suh, and Soong-Hyuck Suh, Mol. Phys. **79**, 1369 (1993).
[16] D. Henderson, J. Chem. Phys. **97**, 1266 (1992).
[17] R. Pospisil, J. Sys, A. Malijevsky, and S. Labik, Mol. Phys. **75**, 261 (1992).
[18] R. Pospisil and A. Malijevski, Mol. Phys. **76**, 1423 (1992).
[19] Y. Zhou and G. Stell, J. Chem. Phys. **89**, 7010; **89**, 7020 (1988); **91**, 3208 (1989).
[20] P. Tarazona, Phys. Rev. A **31**, 2672 (1985); Mol. Phys. **52**, 81 (1984).
[21] G. Stell, Phys. Rev. Lett. **20**, 533 (1968); Phys. Rev. B **2**, 2811 (1970); in *The Equilibrium Theory of Simple Fluids,* edited by H. L. Frisch and J. L. Lebowitz (Benjamin, New York, 1964), Sec. 12.
[22] N. F. Carnahan and K. E. Starling, J. Chem. Phys. **51**, 635 (1969).
[23] W. A. Steele, *The Interaction of Gases with Solid Surfaces* (Pergamon, New York, 1974).
[24] S. Sokolowski and J. Fischer, J. Chem. Soc. Faraday Trans. II **89**, 789 (1993).
[25] A. Gelfand and R. Lipovsky, Phys. Rev. B **36**, 8725 (1987).
[26] R. Hołyst and A. Poniewierski, Phys. Rev. B **36**, 5628 (1987).
[27] R. Pandit, M. Schick, and M. Wortis, Phys. Rev. B **26**, 5112 (1982).